Advanced Production and Industrial Engineering
R.M. Singari and P.K. Kankar (Eds.)

doi:10.3233/ATDE220733

Numerical Analysis of Aerodynamic Drag for the Hyperloop System

Anmol PRABHAKAR[a,1], Arya SHEKHAR[a], Bhuvan JAIN[a], Mohammad ZUNAID[a] and Naushad Ahmad ANSARI[a]

[a] *Department of Mechanical Engineering, Delhi Technological University, Delhi, India*

Abstract. The Hyperloop vehicle is a means of transport in which the pod advances at a fast velocity inside a low-pressure tube to reduce the coefficient of drag. Aerodynamic drag is one of the most significant elements to consider while studying such systems. The design was created on ANSYS SpaceClaim and it consists of a Two-Dimensional model with tapered ends to diminish the drag. Since both ends are tapered, the drag is reduced significantly as compared to the other designs. In this paper, the pod design is analyzed at different speeds, namely 60 ms^{-1}, 120 ms^{-1}, 180 ms^{-1}, 260 ms^{-1}, and 300 ms^{-1} on ANSYS FLUENT and numerical simulations were performed keeping the blockage ratio fixed. Appropriate conditions, equations and k-epsilon turbulence model were applied to produce the desired result. All the drag coefficient values were analyzed, and hence, the graph was plotted. It was observed that the drag coefficient of the pod decreases with an increase in velocity.

Keywords. Hyperloop vehicle; Drag coefficient; Aerodynamic drag

1. Introduction

People's traditional modes of transportation are divided into four categories: road, air, water, and rail. People all across the world are looking for much faster and more efficient ground transportation options as transportation technology has progressed in recent years. The hyperloop is a high-speed land transportation idea that involves passenger pods moving in a partly evacuated tube at transonic speeds [1]. Musk drew the attention of the technical community in 2013 when he proposed the hyperloop concept as a new mode of transportation with performance and comfort benefits for trip distances under 1500 km [2]. Chin et al. introduced the hyperloop concept's general system quantifying the choking risk, which is defined by the throat between the outer tube wall and the pod [3]. The idea is to have a levitating pod that travels inside a low-pressure tube (~100Pa) and at fast speeds (~300 m/s) to minimize the air resistance [4]. Aerodynamic restrictions, such as drag, become major considerations while designing the Hyperloop structure. One of the essential characteristics in the analysis of fast-moving objects, especially within confined tubes (low-pressure), is drag [5][6]. The design of the Hyperloop system is a highly-coupled optimization problem with numerous recursive layout relationships from an engineering viewpoint [7]. Lowering the drag reduces the energy load of the propulsion system.

In this paper, the emphasis is on reducing the drag of the hyperloop structure in comparison with Le et al. [8] by optimizing the design in which both the ends are tapered and omitting the consideration of ideal gas condition and Sutherland model.

2. Methodology

2.1 Designing and details of the model

Previous research looked at the flow attributes of the transonic-speed train entering a tunnel. The two-dimensional axisymmetric model was chosen because it allowed researchers to study a vast parameter space and global patterns [9]. To produce an ideal pod form for two unique goals: increasing lift and lowering drag, a multi-criteria effectivization combined with axisymmetric 2D Computational Fluid Dynamics simulations are applied [10].

As shown in Figure 1, the hyperloop pod was designed aerodynamically on ANSYS SpaceClaim. The dimensions of the pod structure were as follows:

- d_{pod} – 3 m
- d_{tube} – 8 m
- L_{pod} – 55 m
- L_{tube} – 129 m

Here dpod is the diameter of the pod, dtube is the tube's diameter, Lpod is the pod's length, and Ltube represents the length of the tube. Blockage ratio is defined as the projected area of the pod in flow direction to the cross-sectional area of the tube around the pod [11]. The Blockage Ratio is calculated by:

$$B.R = \frac{d_{pod}^2}{d_{tube}^2} \tag{1}$$

The dimensions of the pod were Ø 3m x 55m, and hence, the Blockage Ratio turned out to be 0.140625. The structure shown in Figure 1 was created in 2D and was further used for simulation.

Several research modifying these parameters occur when taking into account the pressure as a variable, the quotient betwixt the cross-sectional area of the capsule and the tunnel (known as Blockage Ratio or BR), and the vehicle speed [12][13].

Figure 1. Geometry of hyperloop pod inside a tube

2.2 Meshing and naming of the model

Firstly, all the labelings of the model were done. While generating the mesh, CFD was selected for Physics Preference as the outcome was a very structured and fine mesh that took into account all the relevant edges and curves in the complex geometry. The element size was 0.05, and the smoothing quality was medium. After the mesh was generated, the total number of nodes and elements were 357,083 and 353,263, respectively.

3. Mathematical Model

In the given research, conservation of mass, conservation of momentum (Navier-Stokes), and energy equations are written sequentially [8][14]:

$$\frac{\partial \rho}{\partial t} + \frac{\partial}{\partial x_i}(\rho u_i) = 0 \tag{2}$$

$$\frac{\partial}{\partial t}(\rho u_i) + \frac{\partial}{\partial x_i}(\rho u_i u_j) = \frac{-\partial P}{\partial x_i} + \frac{\partial}{\partial x_j}[\mu\,(\frac{\partial u_i}{\partial x_j} + \frac{\partial u_j}{\partial x_i} - \frac{2}{3}\delta_{ij}\,\frac{\partial u_k}{\partial x_k})\,] + \frac{\partial}{\partial x_j}(-\rho\{u_i' u_j'\}) \tag{3}$$

$$\frac{\partial}{\partial t}(\rho E) + \frac{\partial}{\partial x_j}[u_j(\rho E\ +\ P)] = \frac{\partial}{\partial x_j}[(k_{eff})\frac{\partial T}{\partial x_j}] + \frac{\partial}{\partial x_j}\left[u_i\mu_{eff}\left(\frac{\partial u_i}{\partial x_j}\right) + \left(\frac{\partial u_j}{\partial x_i}\right) - \frac{2}{3}\delta_{ij}\left(\frac{\partial u_k}{\partial x_k}\right)\right] \tag{4}$$

$$i, j, k = 1, 2, 3$$

Here, P is the fluid pressure, E is the specific internal energy, μ is the fluid viscosity, ρ is the fluid density, k_{eff} is the effective thermal conductivity, μ_{eff} is the effective dynamic viscosity, and u is the fluid velocity.

The turbulence equation used here is the k-Ɛ model because the k-Ɛ model is the most commonly used. Launder and Spalding (1974) produced the "standard" k-Ɛ model, which is one of the most widely used models for indoor and outdoor airflow modeling. The k-Ɛ model can manage a wide range of fluid flow conditions. It has a straightforward structure, delivers outstanding results, and is generally accepted [15].

4. Validation

The numerical analysis by Le et al. [8] was used for validation to confirm the numerical solution's stability. Figure 2 compares the values of the coefficient of drag between our simulation and the work of Le et al. [8] in graphical form. Our work and their work show a similar trend in coefficient of drag, demonstrating that our numerical method is suitable for simulating moving pod-tube configurations. The maximum percentage error in the simulated result is 4%, indicating that the simulated result was validated successfully.

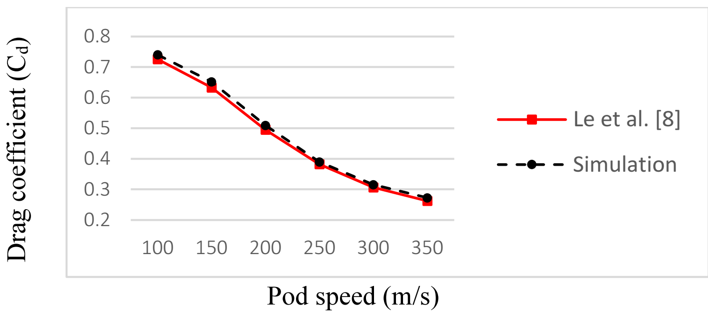

Figure 2. Comparison of drag coefficients between Le et al. [8] and simulation

5. Results

5.1 Parametric Study

The simulation was run on ANSYS Fluent. The units of the pressure were atm, and the solver used here is density-based as it is used for high-speed compressible flows. Gravity is taken into consideration (y = -9.81m/s^2). The energy equation is selected as it represents the conservation of energy of a fluid element. For turbulent flow conditions, the standard k-Ɛ model is commonly used to simulate mean flow characteristics. It is best suited for flow away from the wall. In boundary conditions, five pod speeds were contemplated from 60 ms^{-1} to 300 ms^{-1}. The operating pressure is set at 1/1000 atm, and the operating temperature is 300K. The cross-sectional area of the pod is determined by;

$$A = \frac{\pi d_{pod}^2}{4} \quad (5)$$

and is approximately 7.06858 m^2. The flow behavior upstream is influenced by more than just the inlet boundary condition. The Kantrowitz limit is reached when the inlet is subjected to excessive flow. In reference values, compute from the inlet and insert the area of the pod. Considering the implicit technique can employ a big step size, it is appropriate for solving the calculations that require a lengthy time. Roe FDS was used as a Flux Type, and Least Squares Cell Based was selected as Gradient in Spatial Discretization. Although the first order upwind may get a slighter, less accurate result, it quickly converges and minimizes the computational effort. Pseudo Transient was selected as it helps in stabilizing the case and at the same time gives faster convergence. Afterward, there is a creation of the force report (drag of the vehicle). All the convergence conditions are supposed to be met. Hybrid initialization was used and should be preferred as it accelerates the overall computation. All the contours were kept at the same level in the result.

5.2 Comparative Analysis

Table 1. Drag Coefficients for different velocities of the Hyperloop pod

Velocity (ms^{-1})	**Drag Coefficient (C_d)**
60	0.20603
120	0.18620
180	0.17247
260	0.16414
300	0.16209

The above table (Table 1) records the coefficients of drag for different velocities which came as a result of the simulation. It is evident from the above data that the coefficient of drag decreases with increasing velocity taking area as fixed as mentioned in *5.1*. Here it is observed that at 60 ms^{-1} value of C_d is 0.20603, which further goes down to 0.16209 as velocity equals 300 ms^{-1}. The reason for this phenomenon is that the drag coefficient is inversely proportional to the square of velocity as given in the equation given subsequently:

$$C_d = \frac{D_t}{\left(\frac{1}{2}\right) p v_p^2 A} \tag{6}$$

Compared to open air, the interaction with the tunnel barriers creates extra pressure caused due to the movement of the Hyperloop pod generating additional aerodynamic drag.

Pressure and velocity contours for different velocities are observed. It is evident that the maximum pressure is obtained at the nose of the pod and minimum pressure near the tail. In the case of velocity, the highest magnitude is observed in the spacing between the pod and the tube.

The most accurate result was obtained at a velocity of 300ms^{-1}. The figure given below represents the velocity contour of the same.

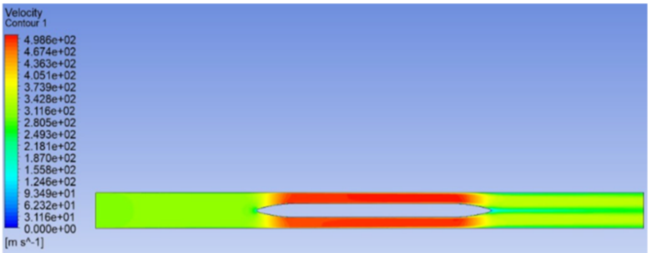

Figure 3: Velocity Contour at $300ms^{-1}$

In Figure 3, the velocity of air is lower at the nose, which eventually becomes greater in the space between the pod and the tube due to the venturi effect, which states that velocity of fluid increases, when passed through constricted and static pressure, decreases similar to the convergence-divergence nozzle.

In their work, Yang et al. [16] found that changing operating speeds and working vacuum pressures had a major impact on the capsule's resistance.

The result obtained by running the simulation is as follows. All the numerical simulations were conducted at different velocities of the pod. Figure 4 indicates that as the drag coefficient decreases, the speed increases.

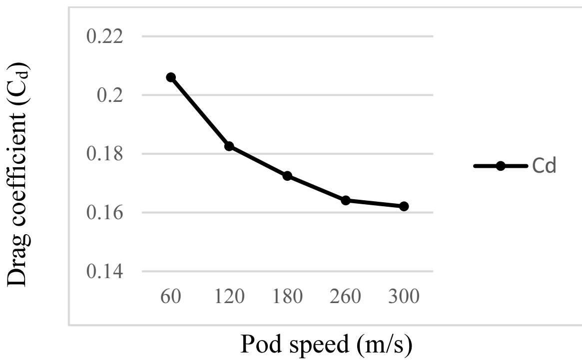

Figure 4. Drag coefficients with respect to velocities of the pod

6. Conclusions

As evident by the results of the present paper and various other research in the domain, the Hyperloop (HL) system emerges as a competitive, powerful, and potential mode of transportation. In the present paper, a Two Dimensional model was created and then analyzed in the hope of optimizing the already existing models. A graph was generated for five different speeds viz. 60 ms^{-1}, 120 ms^{-1}, 180 ms^{-1}, 260 ms^{-1}, and 300 ms^{-1}, and the result indicates that it was possible to converge the coefficient of drag with increasing speed and keeping the blockage ratio constant. The results indicate that when the pod's velocity increases, the coefficient of drag decreases.

Further efforts will target more reduction in drag with minimum dispersal of energy and reduced costs.

7. References

[1] Opgenoord, M.M.J.; Merian, C.; Mayo, J.; Kirschen, P.; O'Rourke.; Izatt, G. MIT Hyperloop Final Project Report; Massachusetts Institute of Technology: Cambridge, MA, USA, 2017.
[2] https://www.tesla.com/sites/default/files/blog_attachments/hyperloop_alpha3.pdf
[3] Opgenoord, M. M. J., Caplan, P. C. (2018). Aerodynamic Design of the Hyperloop Concept. AIAA Journal, 1–10.
[4] Braun, J., Sousa, J., & Pekardn, C. (2017). Aerodynamic Design and Analysis of the Hyperloop. AIAA Journal, 55(12), 4053–4060.
[5] Zhang, Y. (2012). Numerical simulation and analysis of aerodynamic drag on a subsonic train in evacuated tube transportation. Journal of Modern Transportation, 20(1), 44–48.
[6] Pandey, B.K.; Mukherjea, S.K. (2014). Aerodynamic Simulation of Evacuated Tube Transport Trains With Suction at Tail. Volume 12: Transportation Systems.
[7] Kirschen, P.G., Burnell, E. (2021). Hyperloop System Optimization. arXiv: 2104.03907 [cs.CE].
[8] Le, T. T. G., Jang, K. S., Lee, K.-S., & Ryu, J. (2020). Numerical Investigation of Aerodynamic Drag and Pressure Waves in Hyperloop Systems. Mathematics, 8(11).
[9] Li, R., Mei, Y. Study on the Aerodynamic Performance of the High-Speed Train Head with Symmetrical and Asymmetric Nose Shape. In DEStech Transactions on Engineering and Technology Research.
[10] Bizzozero, M., Sato, Y., Sayed, M. A. Aerodynamic study of a Hyperloop Pod equipped with compressor to overcome the Kantrowitz Limit. Journal of Wind Engineering and Industrial Aerodynamics, Volume 218, November 2021.
[11] Lluesma-Rodríguez, F., González, T., & Hoyas, S. (2021). CFD simulation of a hyperloop capsule inside a closed environment. Results in Engineering, 9, 100196.
[12] Kim, T.-K., Kim, K.-H., & Kwon, H.-B. (2011). Aerodynamic characteristics of a tube train. Journal of Wind Engineering and Industrial Aerodynamics, 99(12), 1187–1196.
[13] Li, T., Zhang, X., Jiang, Y., Zhang, W. (2020). Aerodynamic Design of a Subsonic Evacuated Tube Train System. FDMP-Fluid Dynamics & Materials Processing, 16(1), 121-130.
[14] M. Sivapragasam, S. Ramamurthy, M. D. Deshpande, P. White. "An Air Jet Distortion Generation System", 'Hindawi Limited', 2014.
[15] Mishra, P., & Aharwal, K. R. (2018). A review on selection of turbulence model For CFD analysis of air flow within a cold storage. IOP Conference Series: Materials Science and Engineering, 402, 012145.
[16] Yang, Y., Wang, H., Benedict, M., & Coleman, D. (2017). Aerodynamic Simulation of High-Speed Capsule in the Hyperloop System. 35th AIAA Applied Aerodynamics Conference.